

Therapeutic Effect of Bone Marrow Derived Mesenchymal Stem Cells Versus Platelet Rich Plasma on Amiodarone Induced Lung Fibrosis in Adult Male Albino Rat: Histological Study

Wafaa Abd El-Azeem Abdou Boughdady, Zeinab Hegab and Dina Hisham Mohamed

Department of Histology, Faculty of Medicine, Cairo University, Cairo, Egypt

ABSTRACT

Introduction: Lung fibrosis is one of the worldwide progressive serious irreversible diseases. It causes progressive deterioration of lung function and respiratory failure that necessitates lung transplantation. Amiodarone is an effective anti-arrhythmic drug that causes several pulmonary adverse effects; the most serious of which is lung fibrosis. Recently, mesenchymal stem cells (MSCs) and platelet rich plasma (PRP) have emerged as two promising alternative therapeutic tools that can replace organ transplantation with all its drawbacks.

Aim of the Work: To compare the therapeutic effect of bone marrow (BM)-MSCs and PRP on amiodarone induced lung fibrosis in adult male albino rat model.

Materials and Methods: Fifty three adult male albino rats were divided into 4 groups in addition to donor group; those include: group I (control), group II (lung fibrosis) was injected daily with amiodarone (80 mg/ kg) IP for 4 weeks, group III (BM-MSCs) was treated as group II then was injected with a single IV dose of 1 ml of MSCs (3×10^3) and left for 4 weeks and group IV (PRP) was treated as group II then was injected IP with PRP (0.5 ml/kg) twice weekly for 4 weeks. Serum levels of Malondialdehyde (MDA) and transforming growth factor beta (TGF- β) were measured. Lung sections were stained with H&E, Masson trichrome and immunohistochemical stain for alpha smooth muscle actin (α -SMA), Bax and CD68. Also, morphometric and statistical analysis were done.

Results: Group II showed typical histological features of lung fibrosis with abnormal architecture, biochemical and morphometric parameters. While group III & IV showed marked and partial improvement respectively in the histological architecture, biochemical and morphometric parameters.

Conclusion: BM-MSCs proved to be a more promising therapeutic agent for treatment of lung fibrosis than PRP due to their distinctive regenerative, anti-apoptotic and anti-inflammatory effects.

Received: 16 October 2023, **Accepted:** 01 November 2023

Key Words: Amiodarone, BM-MSCs, lung, Fibrosis, PRP.

Corresponding Author: Dina Hisham Mohamed, MD, Department of Histology, Faculty of Medicine, Cairo University, Cairo, Egypt, **Tel.:** +20 11 4300 0698, **E-mail:** dr_dina_hisham@outlook.com

ISSN: 1110-0559, Vol. 47, No. 4

INTRODUCTION

Lung fibrosis is indeed a serious disease of gradual onset distinguished by the increased collagen fibers formation, accumulation of fibroblasts, and architectural changes in the lungs. The condition involves the thickening and scarring of pulmonary tissue, which causes loss of normal lung structure with impaired gas exchange^[1,2,3]. Unfortunately, lung fibrosis is generally considered irreversible, over time, as the fibrosis progresses pulmonary function gradually deteriorates, causing respiratory failure within few years^[4,5].

Lung fibrosis can arise from various factors, including inflammatory lung diseases, hypersensitivity pneumonitis and radiotherapy. Also, certain drugs like bleomycin and amiodarone and viruses as corona virus have been linked to lung fibrosis in addition to some cases with unknown cause^[6,7,8].

The exact mechanisms underlying the development of lung fibrosis are not clear completely, but the release of reactive oxygen and nitrogen radicles may play a role. These toxic substances can elevate transforming growth factor-beta (TGF- β) in various cell types, including macrophages^[9].

Amiodarone is an efficient antiarrhythmic medication^[10]. Though, it can induce many adverse effects on the lung, including pneumonia, alveolar destruction and fatal pulmonary fibrosis through exerting direct toxic effect on lung tissue and creating oxidative stress^[11]. Therefore, we have chosen amiodarone as the agent to induce lung fibrosis in our model.

Nowadays, lung transplantation is the only successful, life-saving therapeutic choice for pulmonary fibrosis and advanced pulmonary disease cases^[12]. However, due to factors such as limited availability of lung donors, high

costs, significant complications, and lower survival rates, lung transplantation is no longer considered the optimal choice for these patients^[12].

Regenerative medicine has emerged as an effective alternative that can overcome the limitations accompanied with organ transplantation. One key component of this field is a group of versatile adult mesenchymal stem cells (MSCs) that exhibit unique abilities for self-maintenance and transdifferentiation into various cell types. MSCs also demonstrate unique regenerative, anti-apoptotic, angiogenic, and anti-inflammatory properties. Furthermore, they have low immunogenicity, meaning they are less likely to cause an immune response, and ethical concerns surrounding their use are minimal. These characteristics make MSCs a prospective therapeutic choice for the treatment of various illnesses^[13,14].

Moreover, platelet-rich plasma (PRP) has evolved as a novel therapeutic strategy that has gained global popularity^[15]. PRP is prepared from a person's own plasma through centrifugation, producing a limited quantity of plasma that contains an elevated level of platelets surpassing the usual levels. It has been applied in various medical fields and is considered a viable alternative for treating several diseases. One of the advantages of PRP is its cost-effectiveness, as it is constructed from the patient's blood. Additionally, the risk of adverse effects and rejection is minimal due to its autologous nature^[10,16].

MATERIALS AND METHODS

Drugs

1. Amiodarone: Cordarone 200mg tablets (Sanofi, Aventis) were converted into powder by grinding, and the calculated dose for each rat was prepared in 1ml polysorbate 80 (El-Gomhoria, Egypt), that is the solvent for amiodarone.
2. Bone marrow Mesenchymal Stem cells (BM-MSCs): Preparation of MSCs from BM: was conducted in the following steps^[17]:
 - Sacrifice and preparation: Three male albino rats, aged 6 weeks, were killed by injecting them IP with phenobarbital (120 mg/kg)^[20]. After sacrifice, the tibia and femur bones were dissected.
 - Flushing and collecting of BM: femur and tibia were rinsed with a mixture of Dulbecco's modified Eagle's medium (DMEM) and 10% fetal bovine serum (FBS). This procedure facilitated the retrieval of the bone marrow.
 - Isolation of nucleated cells from BM: To isolate these cells, A density gradient medium was employed. Density gradient centrifugation allows for the separation of different cell types based on their density.
 - Resuspension and culture medium

preparation: The separated nucleated cells then were suspended in a complete culture medium that was mixed with 1% penicillin-streptomycin. This medium provides the necessary nutrients and growth factors for the cells to grow and proliferate.

- Incubation and primary culture: The resuspended cells were kept in a humidified incubator medium with 5% carbon dioxide at 37 °C. This incubation period lasted for 2 weeks or until enormous colonies of cells were developed. During this time, the cells attached to the culture flask and started proliferating.
- Washing and trypsinization: Once the colonies reached a substantial size and achieved an adequate confluence, the cell cultures underwent a washing process by PBS for 2 times. Following the washes, the cells were treated with a solution of 0.25% trypsin in 1 ml EDTA for a duration of 5 minutes. This trypsin treatment aids in detaching the cells from the surface of the culture flask.
- Resuspension and second-passage culture: The separated cells were trypsinized, then resuspended in a medium that contained serum and incubated in a brand-new culture flask (50 cm²). This step represents the first passage of the cell culture.
- Identification of MSCs: The identification of MSCs was performed based on their morphological characteristics. MSCs typically have a fusiform (spindle-shaped) morphology and exhibit adhesiveness to surface of culture.

Labeling of stem cells with PKH26 dye:^[18]

A fluorescent dye called Paul Karl Horan-26 (PKH-26) (Sigma company, Egypt) was used to label MSCs that were obtained from the second passage to trace homing of stem cells in the lung. The cells were pelleted, washed in a medium devoid of serum, and then labeled. Once labeled, the MSCs were injected into the rats via the tail vein using a sterile syringe and saline solution. Rats were sacrificed 3 days after MSCs injection and the injected cells were then examined in unstained lung sections under a fluorescent microscope for visualizing and tracking their presence, as indicated by the PKH26 red fluorescence.

Injection of MSCs: rats in group III were administered labeled MSCs that had been mixed with one ml saline. The mixture was aspirated into a sterilized needle with a volume of 1 ml and injected into each rat via the tail vein.

Platelet rich plasma (PRP)

Five donor rats were used to collect 3 ml of blood each,

by a sterilized needle that contained 0.3 ml of sodium citrate. A sterilized falcon tube was used to hold the collected blood. To separate desired components, a seven minutes centrifugation of the citrated blood was performed at 3000 rpm (revolutions per minute). Buffy coat, including leukocytes and platelets, was carefully removed from the supernatant after centrifugation and transferred to a second sterilized falcon tube. For a second occasion, a five minutes centrifugation was carried out at 4000 rpm. This process resulted in the formation of platelet pellet at the bottom of the tube, representing PRP^[19].

Both BM-MSCs and PRP were prepared in laboratory of Biochemistry Department, Faculty of medicine, Cairo University.

Animals

This study included 53 adult male albino rats (150-200 gm. BW) (8 rats used as donor rats, the remaining 45 rats were used in the experiment). The rats were kept in appropriate well-ventilated wire cages at room temperature. They were provided with water and food freely. Throughout the study, all procedures were performed according to the ethical rules of Cairo University-Institutional Animal Care and Use Committee (CU-IACUC) (Approval number [CU III F 43 23]).

Experimental design

Donor group: 8 rats, used to obtain MSCs and PRP as mentioned above.

Four groups were created at random from the remaining 45 rats:

Group I (Control Group): 15 animals, received the drug solvent via the same route of administration and for the same experimental periods as the corresponding experimental groups.

It was subsequently separated into three identical subgroups, each with five rats:

- Subgroup Ia: corresponding to group II, Rats were IP injected with 1 ml of polysorbate 80 (vehicle of amiodarone) for four weeks before being sacrificed.
- Subgroup Ib: corresponding to group III, rats received the same treatment identically with subgroup Ia for the same period, after that, injected once with 1ml PBS (vehicle of stem cells) intravenously (IV) through tail veins (after completion of amiodarone injections) then sacrificed after four weeks.
- Subgroup Ic: corresponding to group IV, rats received the same treatment identically with subgroup Ia for the same period, after that, injected with 1ml sodium citrate (vehicle of PRP) IP (after completion of amiodarone injections) twice/week for four weeks then sacrificed.

The other 30 rats were allocated evenly in the form of 3 experimental groups (each with 10 animals):

Group II (Lung fibrosis): animals were injected daily with amiodarone (80 mg/ kg) IP for four weeks^[10] then sacrificed to confirm induction of lung fibrosis.

Group III (BM-MSCs): Animals received the same treatment identically with group II for the same period, after that, injected once with IV dose of 1 ml of MSCs (3×10^3)^[11], (after completion of amiodarone injections) through tail vein and sacrificed after four weeks (except for 2 rats sacrificed 3 days after MSCs injection to trace homing of PKH- labelled MSCs in the lung tissue).

Group IV (PRP): Animals received the same treatment identically with group II for the same period, after that, injected IP with PRP (0.5 ml/kg)^[10], (after completion of amiodarone injections) twice /week for four weeks then sacrificed.

Experimental procedure

Biochemical Study: two ml of venous blood were taken from each animal at the conclusion of experiment, just before sacrifice to assess serum level of malondialdehyde (MDA) and transforming growth factor beta (TGF- β). These investigations were performed at laboratory of Biochemistry Department, Kasr Al-Aini Faculty of Medicine, Cairo University by radioimmunoassay (RIA)

Histological Study: To sacrifice animals after completion of experiment, they received IP phenobarbital (120 mg/kg)^[20]. The lungs were dissected out, cut and specimens were quickly put in 10% formol saline for fixation and immersed in paraffin blocks. Subsequently, sections of about 7 μ m thickness were cut and exposed to the following:

Light microscopic study

- a. Hematoxylin and Eosin (H and E) stain^[21].
- b. Masson Trichrome stain^[22].
- c. Immunohistochemical staining^[22] for:
 - α -SMA: A marker for fibrosis. The primary antibody was a rabbit polyclonal antibody (ABT1487, Sigma company, Egypt). α -SMA positive cells showed brown cytoplasmic deposits.
 - Bax: Proapoptotic member of Bcl-2 family which promotes cell death through direct interactions with the proapoptotic members^[23]. Bax primary antibody was a mouse monoclonal antibody (Labvision, Thermoscientific, USA). Bax positive cells showed brown cytoplasmic deposits.
 - CD68: A marker for macrophages. CD68 primary antibody was a mouse monoclonal antibody (Cell Marque. Rocklin, CA. USA). CD68 positive cells showed brown cytoplasmic deposits.

To do immunostaining, the tissue sections underwent antigen unmasking by boiling them in a 10 mM citrate

buffer (Cat. No, AP 9003) with a pH of 6. This boiling process lasted for 10 minutes. Subsequently, the sections were allowed twenty minutes to cool at RT. Next, sections were exposed to primary antibodies for a duration of 1 hour. For immunostaining, the Ultravision detection system (Cat. No, TP-015-HD) was employed. After that, Mayer's hematoxylin stain (Cat. No, TA-125-MH) was used to counterstain the sections. The used materials were procured from Lab Vision Thermo Scientific, California, USA.

Fluorescent microscopic study: In group III (BM-MSCs group), sections that were not subjected to stain belonging to rats sacrificed 3 days after MSCs injection were investigated using fluorescent microscope.

Morphometric Study

Image analysis was set up using Leica Qwin 500 C" image analyzer computer system (Cambridge, England) at Histology Department, Faculty of Medicine, Cairo University. Alveolar surface area, number of pneumocyte type II, area percent of collagen fibers and positive immunoreactivity for α -SMA and Bax and number of CD68 positive macrophages were calculated in the related sections in 10 fields without overlap from different sections belonging to each group separately ($\times 400$).

Statistical Analysis

It was done for whole morphometric and biochemical findings using SPSS software update 21 and presented as mean \pm standard deviation (SD). To do comparison between various groups, ANOVA test was employed, then a post hoc Tukey test was done. Statistical significance was determined by evaluating the p-value, and differences were deemed of statistical significance when the p-value was lower than 0.05^[24].

RESULTS

General comments

No morbidity or mortality was reported throughout the study in any group. The results of control subgroups were identical, so they were presented as the control group.

Biochemical results

Mean values of MDA and TGF- β level in serum were significantly increased in lung fibrosis group versus the control, BM-MSCs and PRP treated groups. However, PRP group recorded a significant increase of these levels versus control and BM-MSCs groups (Table 1).

Histological results

Haematoxylin and Eosin results

Lung sections of control rats displayed typical histological configuration; alveoli and alveolar sacs were patent, with thin alveolar septa and the lining of bronchioles exhibited columnar cells and Clara cells. The alveolar lining revealed predominant flat nucleated squamous cells (pneumocytes I) and few large cuboidal cells

displaying spherical nuclei (pneumocytes II). Pulmonary blood capillaries were noticed in the alveolar septa (Figures 1 a,b).

Lung sections of group II (Lung fibrosis) revealed loss of normal architecture, presented by consolidation of large areas of lung tissue, collapsed alveoli with greatly thickened alveolar septa. The lumen of bronchioles contained detached epithelial cells. Alveoli were mainly lined by pneumocyte type II cells. Numerous fibroblast cells in addition to many pneumocytes II were noticed in thickened interalveolar septa. Some pneumocyte type II cells aggregated in the form of acini. Thickened wall of pulmonary blood vessels and heavy inflammatory cell infiltration between the alveoli as well as around the bronchiolar adventitia were observed. In addition, fluid exudates, extravasation of RBCs in the thickened septa were seen (Figures 2 a-d).

In group III (BM-MSCs treated group), lung sections demonstrated nearly normal lung appearance. The alveoli were patent, mostly separated by thin septa containing blood capillaries. Alveolar lining illustrated more pneumocyte I and less pneumocyte II compared to group II. Occasional partially collapsed alveoli were noticed. The bronchioles appeared normal (Figures 3 a,b).

While sections of group IV (PRP treated group) illustrated partial histological improvement compared to lung fibrosis group. Some alveoli appeared patent with thin interalveolar septa, while others were collapsed or partially collapsed and separated by thickened interalveolar septa. The alveolar lining exhibited predominant pneumocyte II with few pneumocyte type I cells. The thickened interalveolar septa exhibited many fibroblasts and pneumocyte type II cells with extravasated RBCs. There were some separated epithelial cells visible in the bronchioles' lumen. In addition, moderate inflammatory cell infiltration around some bronchiolar adventitia and thick wall of some blood vessels were noticed (Figures 3 c,d).

Masson trichrome results

Control and BM-MSCs groups illustrated scanty collagen fibers in lung interstitium. While lung fibrosis group illustrated heavy collagen fibers distribution in the interstitium. Concerning PRP treated group, moderate amount of collagen fibers was noticed in lung interstitium (Figures 4 a-d).

Alpha-SMA Immunostaining

The control group illustrated negative cytoplasmic α -SMA immunoreaction in the alveolar lining cells. While lung fibrosis group demonstrated strong positive cytoplasmic immunoreaction in abundant fibroblasts and pneumocytes type II. BM-MSCs treated group revealed faint positive cytoplasmic immunoreaction. Concerning PRP treated group, strong positive cytoplasmic immunoreaction was noticed in multiple fibroblasts and pneumocytes type II (Figures 5 a-d).

Bax Immunostaining

Control sections illustrated mild cytoplasmic Bax immunopositivity in few type I and type II pneumocytes. While lung fibrosis group demonstrated widely distributed severe positive cytoplasmic Bax immunoreactivity. BM-MSCs treated group showed mild positive cytoplasmic Bax immunoreaction in some type I and type II pneumocytes. Regarding PRP treated group, sections showed strong positive cytoplasmic Bax immunoreaction in numerous cells (Figures 6 a-d).

CD68 Immunostaining

Control and BM-MSCs groups revealed few numbers of macrophages with positive CD68 immunoreaction. This number was highly increased in the lung fibrosis group and moderately increased in PRP treated group (Figures 7 a-d).

Fluorescent microscopic results

Fluorescent microscopic examination of unstained sections related to BM-MSCs group by the illustrated red

colored fluorescence of BM-MSCs labelled with PKH-26 in lung interstitium (Figure 8).

Quantitative morphometric results

Mean alveolar surface area of Lung fibrosis group recorded a significant descent versus control, BM-MSCs and PRP groups. PRP treated group also revealed significantly low alveolar surface area in comparison with control and BM-MSCs groups. Lung fibrosis group showed significantly high number of pneumocytes II, area percent of collagen fibers, area percent of positive Bax immunoreactivity and number of macrophages with positive CD68 immunoreactivity versus the control, BM-MSCs and PRP groups. PRP group also showed a significant elevation in these values when compared to control group and BM-MSCs group. Control group demonstrated negative immunoreactivity for α -SMA. Lung fibrosis group recorded a significantly elevated immunoreaction of α -SMA in comparison with control, BM-MSCs and PRP groups. PRP group also displayed a significant increase in this value versus control and BM-MSCs groups (Table 2).

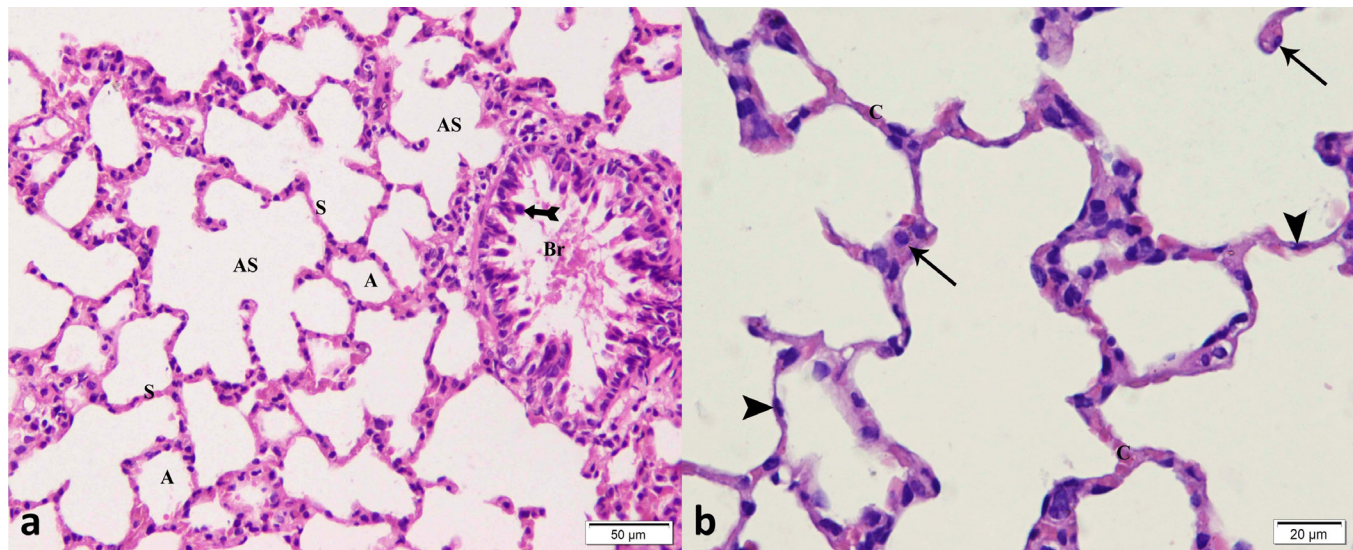


Fig. 1: Photomicrographs control group H and E lung sections (a,b) showing: a: Patent alveoli (A) and alveolar sacs (AS), exhibiting thin interalveolar septa (S) and a normal bronchiole (Br) having columnar and Clara cells (double headed arrow) in their lining (x 200). b: Alveolar lining shows predominant flat nucleated pneumocyte I (arrowheads) and less pneumocyte II exhibiting spherical nuclei (arrow). Note pulmonary blood capillaries (C) in the interalveolar septa (x 400).

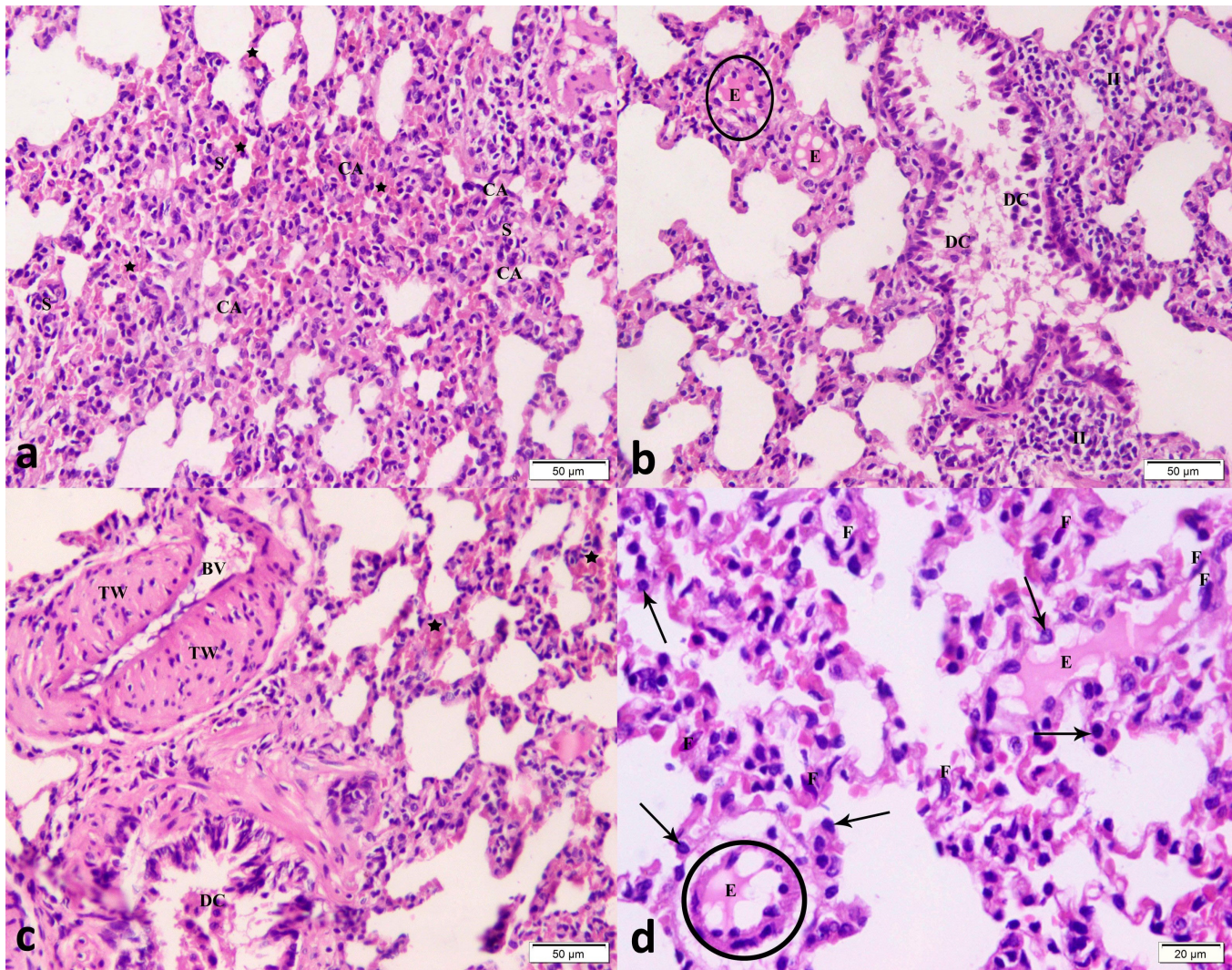


Fig. 2: Photomicrographs of Hand E sections of lung fibrosis group (a,b,c and d) illustrating a: Consolidated part with collapse of the alveoli (CA), marked thickness of interalveolar septa (S) and extravasation of RBCs (stars) in the lung interstitium between the alveoli (x 200). b: A bronchiole containing detached epithelial cells (DC) in its lumen, heavy inflammatory cellular infiltration (II) around the adventitia of the bronchiole, some pneumocyte type II cells forming acini (circle) around fluid exudate (E) (x 200). c: A pulmonary blood vessel (BV) with very thickened wall (TW). Note Detached epithelial cells (DC) in the lumen of a bronchiole and extravasated RBCs (stars) between the alveoli (x 200). d: Alveolar lining exhibits pneumocytes II (arrows) mainly. Thickened interalveolar septa exhibiting many fibroblast cells (F) in addition to increased number of pneumocytes type II (arrows). Note pneumocyte type II formed an acinus(circle) with fluid exudate (E) (x 400).

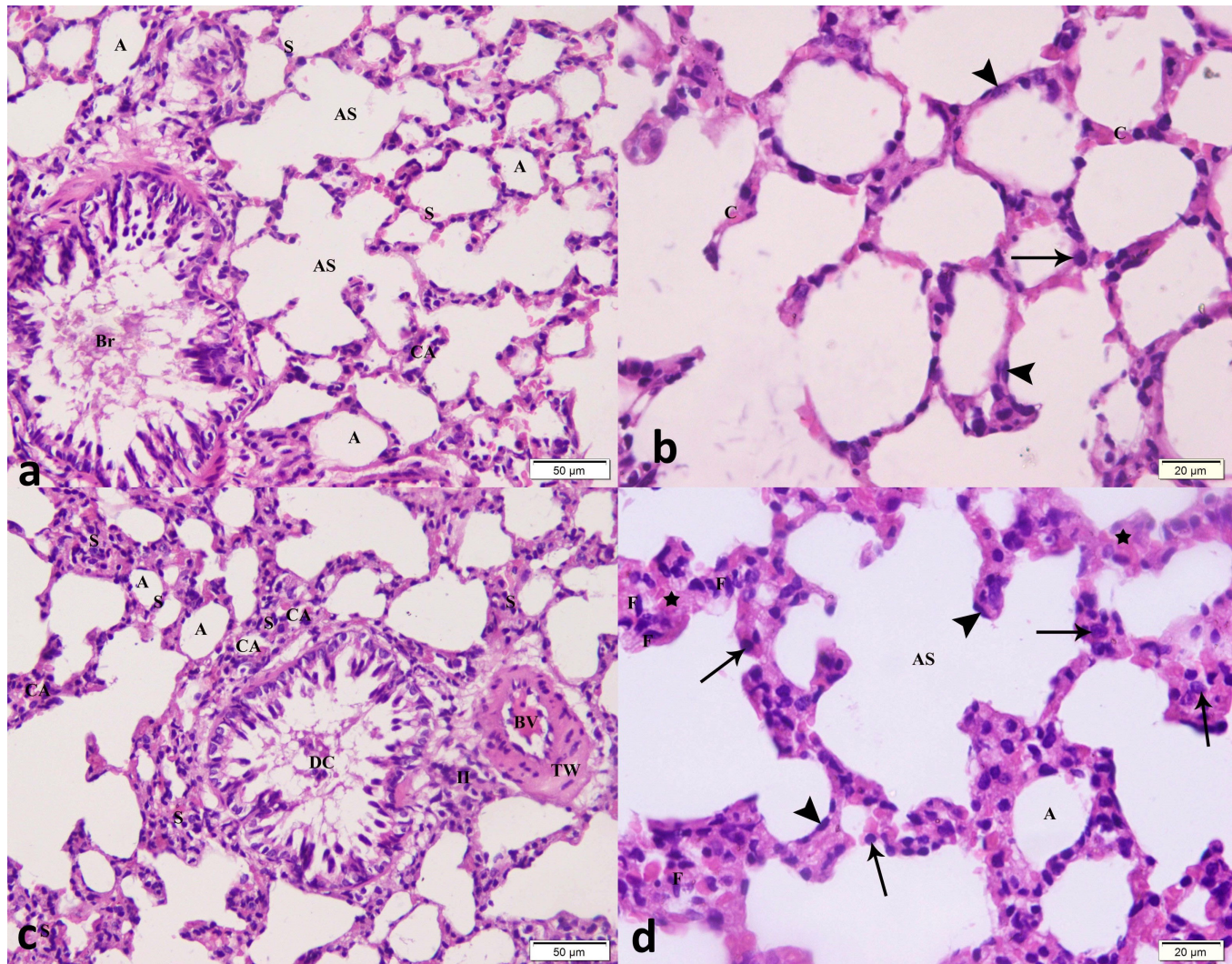


Fig. 3: Photomicrographs of H&E sections of BM-MSCs group (a,b) demonstrating: a: Patent alveoli (A) and alveolar sacs (AS), thin alveolar septa (S) and a normal bronchiole (Br). Note occasional partially collapsed alveoli (CA) (x 200). b: Alveolar lining mostly display pneumocyte I (arrowheads) and few pneumocyte type II cells (arrow). The interalveolar septa exhibit pulmonary blood capillaries (C) (x 400). PRP treated group (c,d) showing c: Some alveoli (A) are patent with thin interalveolar septa (S) while others appear collapsed or partially collapsed (CA) with thickened interalveolar septa (S). Detached Epithelial cells (DC) are seen in the lumen of a bronchiole. Note moderate inflammatory cellular infiltration (II) around the adventitia of a bronchiole and moderately thickened wall (TW) of a pulmonary blood vessel (BV) (x 200). d: Alveoli (A) and alveolar sacs (AS) lining reveal mainly pneumocyte II (arrows) with few pneumocyte I (arrowheads). The thickened septa exhibit many pneumocytes type II (arrows) and fibroblasts (F) in addition to extravasated RBCs (stars) (x 400).

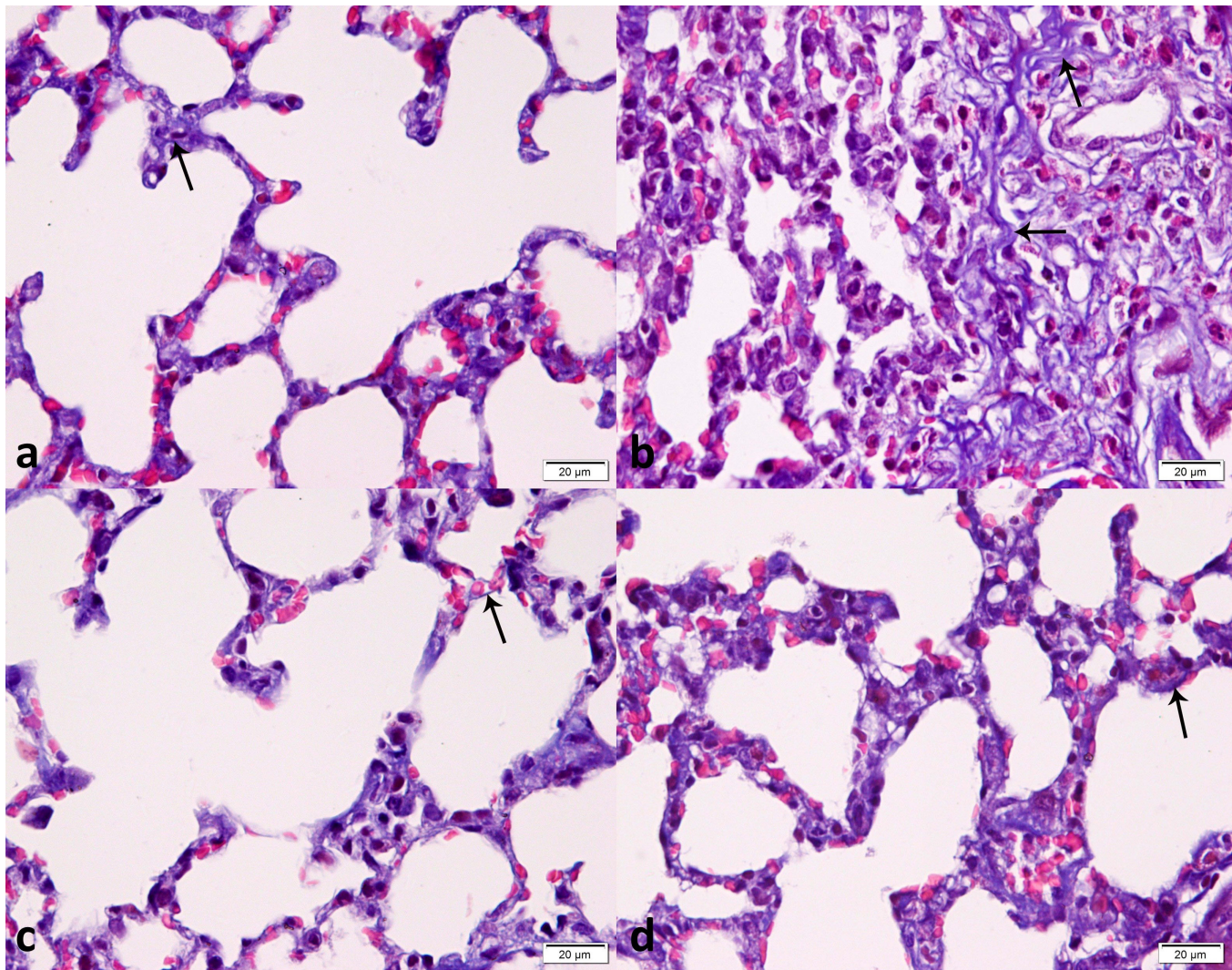


Fig. 4: Photomicrographs belonging to lung sections stained with Masson trichrome revealing: a: Control group a and c: BM-MSCs treated group demonstrating scanty collagen fibers (arrow) in lung interstitium. b: Lung fibrosis group demonstrating heavy distribution of collagen fibers (arrows) in lung interstitium. d: PRP treated group showing moderate collagen fiber amount (arrow) in lung interstitium (x 400).

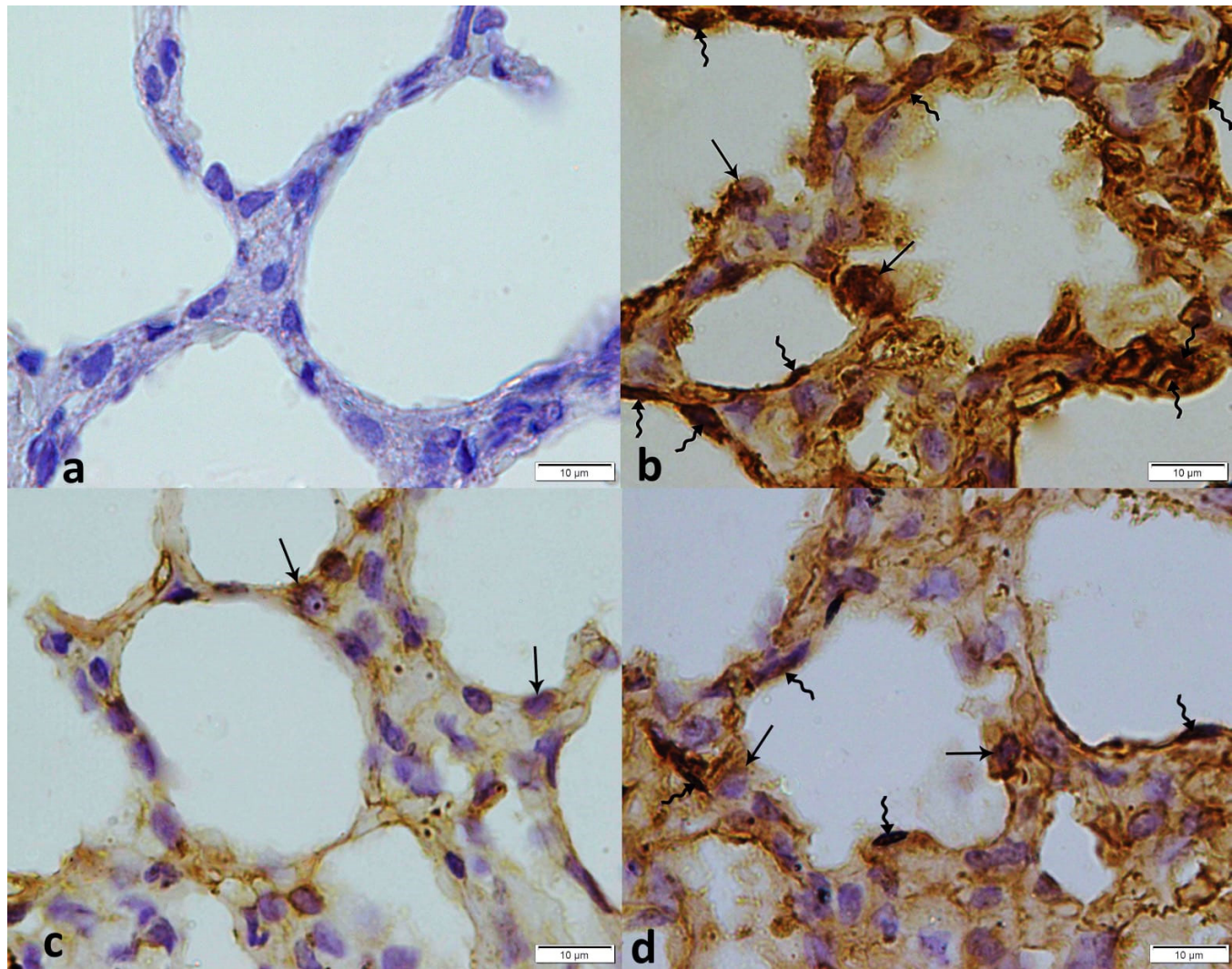


Fig. 5: Photomicrographs of lung sections immunostained with α SMA showing: a: Control group showing negative cytoplasmic α SMA immunoreaction in the alveolar lining cells. b: Lung fibrosis group revealing strong positive cytoplasmic immunoreaction in abundant fibroblasts (wavy arrows) and pneumocytes type II (arrows). c: BM-MSCs treated group demonstrating faint positive cytoplasmic immunoreaction in some pneumocytes type II (arrows). d: PRP treated group demonstrating strong positive cytoplasmic immunoreaction in multiple fibroblasts (wavy arrows) and pneumocytes type II (arrows) (x 1000).

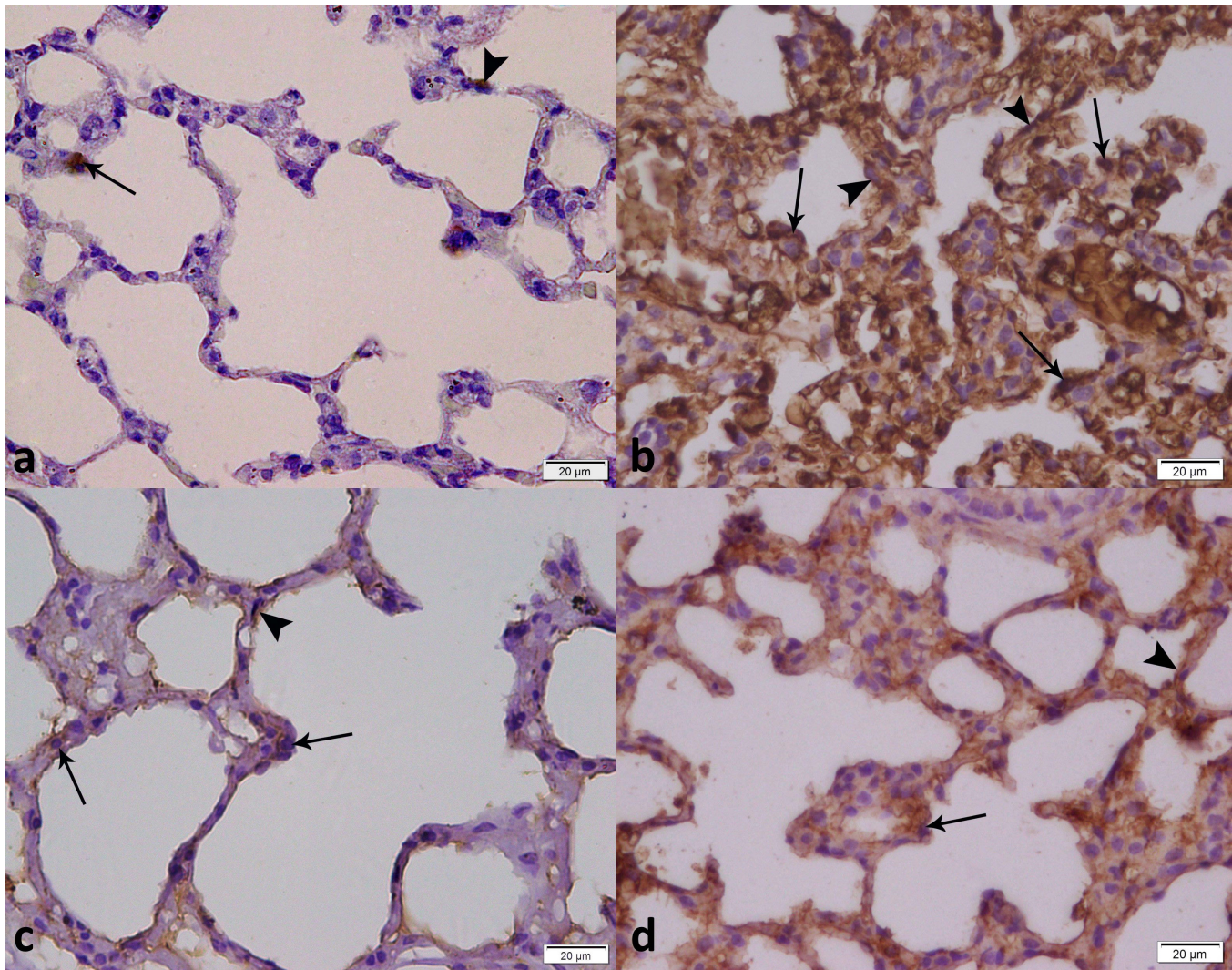


Fig. 6: Photomicrographs of Bax stained sections displaying: a: Control sections showing mild positive cytoplasmic Bax immunoreaction in few pneumocytes type I (arrowhead) and type II (arrow). b: Lung fibrosis group demonstrating widely distributed severe positive cytoplasmic Bax immunoreaction in pneumocytes I (arrowheads) and pneumocytes II (arrows). c: BM-MSCs treated group revealing mild positive cytoplasmic Bax immunoreaction in some pneumocytes I (arrowhead) and pneumocytes II (arrows). d: PRP treated group demonstrating strong positive cytoplasmic Bax immunoreaction in numerous pneumocytes I (arrowhead) and pneumocytes II (arrow) (x 400).

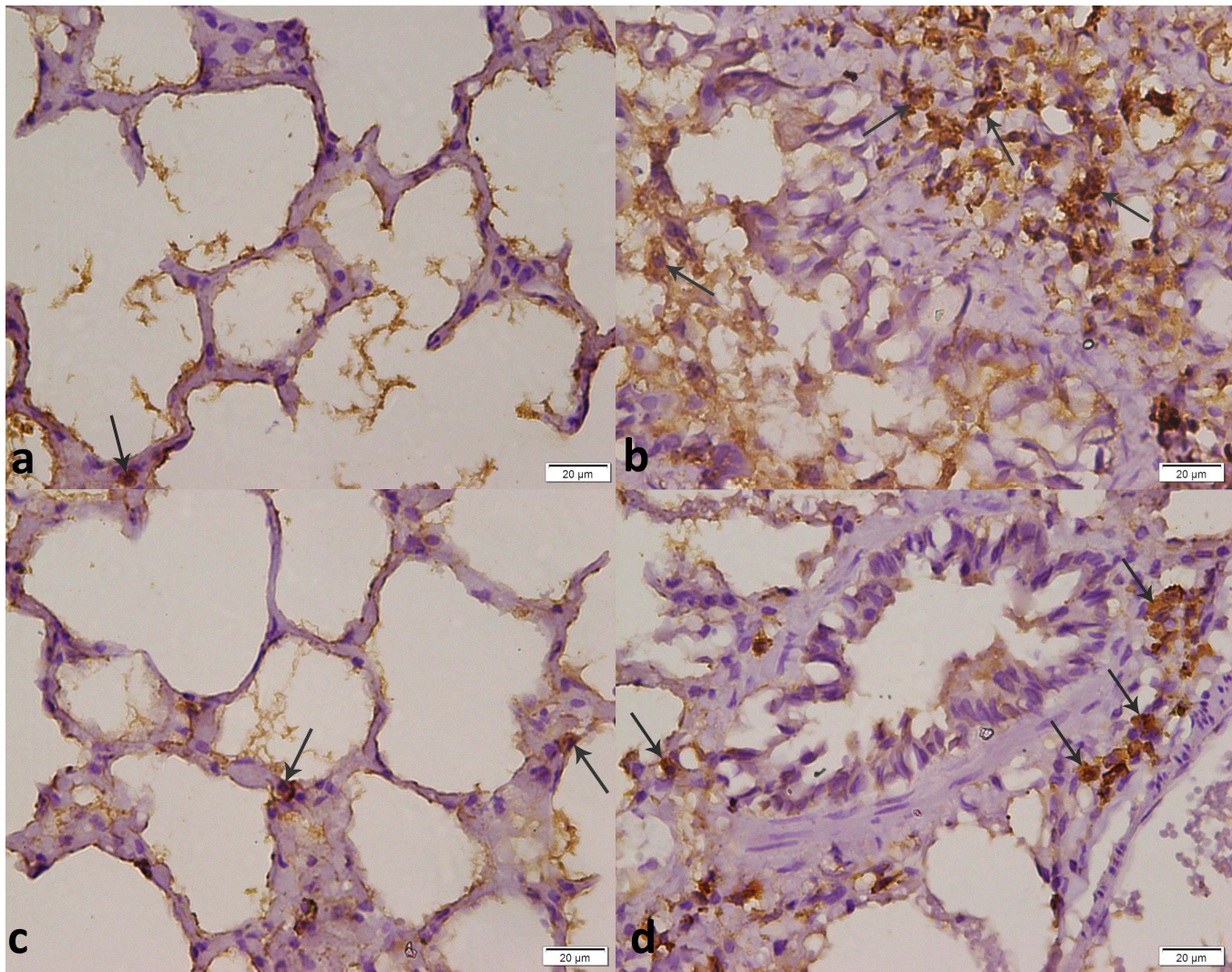


Fig. 7: Photomicrographs of CD68 sections showing: a: Control group and c: BM-MSCs treated group demonstrating few macrophages with positive CD68 immunoreaction (arrows). b: Lung fibrosis group showing highly increased number of macrophages with positive CD68 immunoreaction (arrows) d: PRP treated group illustrating moderately increased number of macrophages with positive CD68 immunoreaction (arrows) (x400).

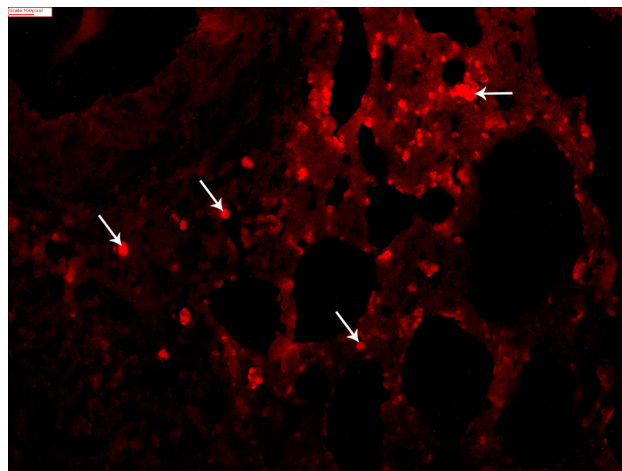


Fig. 8: Photomicrograph of lung unstained section related to group III (BM-MSCs group) demonstrating red colored fluorescence of homed MSCs labelled with PKH-26 in lung tissue (PKH26 fluorescent dye, (x 200).

Table 1: Mean values ± SD of Serum MDA and TGF-β levels in the experimental groups

	Control	Lung fibrosis	BM-MSCs	PRP
Serum MDA	5.63 ± 1.19	9.27 ± 1.22 ^{acd}	6.25 ± 1.15 ^{bd}	7.92 ± 0.85 ^{abc}
Serum TGF-β	4.57 ± 0.75	10.28 ± 1.09 ^{acd}	4.33 ± 1.72 ^{bd}	6.1 ± 1.21 ^{abc}

a Significantly different versus control group at $P < 0.05$
 b Significantly different versus group II at $P < 0.05$
 c Significantly different versus group III at $P < 0.05$
 d Significantly different versus group IV at $P < 0.05$

Table 2: Mean values ± SD of morphometric parameters in the experimental groups.

	Control	Lung fibrosis	BM-MSCs	PRP
Alveolar surface area	2093 ± 7.4	247.5 ± 9.7 ^{acd}	2088 ± 14.4 ^{bd}	1659 ± 7.4 ^{abc}
Mean no. of pneumocytes type II	2.6 ± 0.91	8.7 ± 0.87 ^{acd}	3.1 ± 0.72 ^{bd}	4.87 ± 1.05 ^{abc}
Area % of collagen fibres	3.76 ± 0.47	12.79 ± 1.43 ^{acd}	3.58 ± 0.67 ^{bd}	4.96 ± 0.67 ^{abc}
Area % of Bax +ve immunoreactivity	3.02 ± 0.01	8.14 ± 1.5 ^{acd}	3.19 ± 0.67 ^{bd}	4.36 ± 0.48 ^{abc}
Area % of α-SMA +ve immunoreactivity	0.00 ± 0.00	9.46 ± 1.06 ^{acd}	1.35 ± 0.47 ^{bd}	6.77 ± 1.05 ^{abc}
Mean no. of macrophages with positive CD68 immunoreactivity	1.6 ± 0.18	23.2 ± 1.23 ^{acd}	2.4 ± 0.9 ^{bd}	10.5 ± 1.44 ^{abc}

a Significantly different versus control group at $P < 0.05$
 b Significantly different versus group II at $P < 0.05$
 c Significantly different versus group III at $P < 0.05$
 d Significantly different versus group IV at $P < 0.05$

DISCUSSION

Tissue fibrosis is linked to global morbidity and mortality^[25]. Pulmonary fibrosis; in particular, is a condition with poor prognosis and limited treatment options. However, recent advancements in alternative therapies including the use of MSCs and PRP have revealed encouraging outcomes in the management of pulmonary fibrosis^[26,27]. Therefore, this study aimed at comparing the therapeutic effectiveness of these two therapies in ameliorating a model of pulmonary fibrosis elicited by amiodarone drug in rats.

In this work, fibrosis of lung was conducted via amiodarone injection. As amiodarone possesses lipophilic properties, it tends to accumulate in various tissues and interact with the phospholipids present^[28]. Consequently, the pathogenesis of amiodarone induced lung fibrosis is dependent on the cumulation of phospholipid complexes within tissue macrophages and type II pneumocytes. Moreover, studies by Hasan *et al.* in 2016^[29] and Gawad *et al.* in 2018^[30] have associated lung toxicity induced by amiodarone with high emission of ROS hence damaging membrane lipids.

Malondialdehyde (MDA) represents the end product of peroxidation occurring in polyunsaturated fatty acids. Its level serves as a widely recognized indicator for oxidative stress^[31]. The data from the present study demonstrated significantly elevated serum MDA levels in the lung fibrosis group versus both the control group and all experimental groups, thereby indicating the presence of oxidative stress. These findings align with the observations made by Maher *et al.*, 2020^[10].

In cases of acute lung insult, alveolar epithelial breakdown typically leads to subsequent destruction of the normal structure of the alveoli as well as the discharge of various inflammatory cells, which consequently activate immune reaction^[32]. Inflammation usually serves as the initial step of the tissue repair response. However, if inflammation persists, it ultimately terminates in fibrosis^[33]. Development of fibrosis was morphometrically assessed by sections stained by Masson trichrome, which demonstrated statistically significant expression of collagen in lung fibrosis group versus that of the control and all experimental groups.

In lung fibrosis group, H and E sections uncovered the loss of normal architecture, characterized by the consolidation of diffuse regions of lung tissue and collapsed alveoli accompanied by marked thickening of alveolar septa. The bronchiole lumens contained detached epithelial cells. The alveolar lining mostly displayed pneumocyte II cells. The septa between alveoli revealed an increased number of fibroblast cells as well as pneumocyte type II cells. These findings were similar to those of Al-Shammari *et al.*, 2016^[34], Gawad *et al.*, 2018^[30], and Moustafa *et al.*, 2020^[35]. Additionally, some pneumocyte II cells aggregated in the form of acini, potentially indicating that they try to engage in repair processes which is in harmony with Anversa *et al.*, 2011^[36], who identified pneumocyte II cells to be local progenitor cells capable of regeneration and restoration of respiratory tract epithelium.

Examination revealed a thickened wall of pulmonary blood vessels with heavy cellular invasion of inflammation. Additionally, expanded septa displayed fluid exudates and extravasation of red blood cells. It was established that in

cases of fibrosis, pulmonary capillaries, particularly those located in fibrous areas, exhibited an increased collagen genes expression, which actively participates in secretion of extracellular matrix^[37]. Moreover, within fibrotic tissues, the robust proliferation of fibroblasts induces abnormal angiogenesis to meet the nutritional demands of these dividing fibroblasts^[38].

Numerous studies have thoroughly documented engagement of various cell types in the initiation of fibrosis process in lung. The prominent players in this complex process include epithelial lining cells, macrophages, and fibroblasts^[39]. Notably, pneumocytes are responsible for a main part in development of lung fibrosis^[40]. Both pneumocyte type I, II are crucial in maintaining the proper structure of the alveolar wall. When pneumocyte I die due to any pathology, the compensatory response typically involves the proliferation and differentiation of pneumocyte II into pneumocyte I, ensuring integrity of the alveoli^[41]. However, in the context of lung fibrosis, chronic injury triggers the apoptosis of pneumocyte I, leading to their subsequent loss and the hyperplasia of pneumocyte II. Contrary to their regenerative role, these pneumocyte II begin to release an array of inflammatory cytokines. Consequently, these cytokines contribute to the pathogenic activation and proliferation of fibroblasts together with an enhanced deposition of collagen and subsequent alveolar collapse^[42]. Furthermore, under pathological conditions, the epithelial mesenchymal transition (EMT) serves as well-known reservoir of myofibroblasts^[43]. This phenomenon can explain the significantly increased positive cytoplasmic α -SMA immunoreactivity observed in abundant fibroblasts and pneumocytes II in sections of lung fibrosis group in contrary with MSCs and PRP treated groups in current study.

Among the most important profibrotic cytokines comes TGF- β 1 exerting its influence on lung fibrosis through the activation of macrophages and fibroblasts, subsequently leading to the deposition of extracellular matrix. Additionally, TGF- β 1 triggers conversion of fibroblasts giving rise to myofibroblasts. Added to that, it was discovered that TGF- β 1 encourages production of extracellular matrix by upregulating certain profibrotic genes, like α -SMA^[44]. This could explain findings regarding serum levels of TGF- β 1 in this work, which showed significantly high levels in lung fibrosis group in comparison to control group and all experimental groups. It also supports the results of the current study regarding immunostaining with α -SMA antibodies, that showed significantly intense staining of lung sections in the lung fibrosis group versus the control group and all experimental groups.

Moreover, it has been documented that TGF- β 1 stimulation contributes to epithelial cells apoptosis, and as long as TGF- β 1 production persists, epithelial cell injury continues. This finding goes parallel with the results obtained in this study, where immunostaining with Bax antibodies showed significantly intense staining of lung

sections in the lung fibrosis group versus the control group and all experimental groups. Bax; apoptotic protein, exerts a notable influence on mitochondrial-dependent apoptosis. It was documented that Bax induces epithelial cell death while simultaneously promoting fibroblast proliferation in cases of idiopathic lung fibrosis. Notably, oxidative stress has been recognized as a pivotal factor in the activation of Bax^[45].

On the other hand, within an inflammatory microenvironment, the release of various cytokines can stimulate different intracellular signaling pathways in macrophages, ultimately leading to an increased expression of macrophage associated polarization markers. This, in turn, stimulates macrophages trans-differentiation into two distinct phenotypes: M1 (pro-inflammatory), which produce inflammatory mediators, and M2 macrophages (pro-fibrotic), which generate pro-fibrotic factors^[46]. This is supported by immunohistochemical results in the current study regarding immunostaining with CD68 antibodies, one of the macrophage polarization markers that showed significantly intense staining in fibrosis group versus the control group and all experimental groups. This agreed with Hamam *et al.*, 2019^[47] who noted significantly increased mean number of CD68-positive cells in cases of lung fibrosis induced by CCL4 versus control and MSCs treated groups.

Treatment with MSCs demonstrated significant improvement in all investigated parameters compared to lung fibrosis group and PRP treated group. The data from this group exhibited results that were nearly comparable to those of control group. In H and E stained sections, alveolar majority was maintained patent and had thin septa containing blood capillaries. The alveoli exhibited more pneumocytes I and less pneumocytes II when compared to lung fibrosis group. Occasional partially collapsed alveoli were noticed. The bronchioles appeared normal. Masson trichrome stained lung sections from the BM-MSCs treated group revealed that homed BM-MSCs significantly alleviated lung fibrosis with markedly reduced collagen deposition between the alveoli. Similar findings were also reported by Sabry *et al.*, 2014^[48] and Zakaria *et al.*, 2021^[7].

Masson trichrome lung sections and H and E stained sections related to MSCs group supported our findings showing significant reduction in collagen expression in the former, increased surface area of the alveoli and decreased number of pneumocytes II in the latter in comparison to those of lung fibrosis and PRP groups.

A further support to previous findings came from serum levels of MDA and TGF-B1, where the difference was negligible between MSCs and control groups while it showed significant reduction in both relative to both lung fibrosis group and PRP treated group suggesting a more potent antioxidant and antifibrotic effect for BM-MSCs versus PRP.

Furthermore, the immunohistochemical results aligned with the other findings of this study. Immunostaining

with Bax, α -SMA, and CD68 antibodies revealed that the difference was non-significant between BM-MSCs and control groups. However, a significant reduction was observed compared to both lung fibrosis and PRP group.

Various mechanisms have been reported regarding the repair of damaged lung tissue by BM-MSCs. In a bleomycin lung fibrosis mice model, the homed MSCs acquired characteristics of pneumocyte type I cells at both the molecular and morphological levels. MSCs can also transform into pneumocyte type II cells, which can alleviate lung inflammation and fibrosis, and promote healing. Sabry *et al.*, 2014^[48], stated that fibrosis resolution is accelerated through epithelial restitution, and added that stem cells renovate the organization of the cytoskeleton of the alveolar epithelium. Moreover, MSCs facilitate the regeneration of endothelial cells and restoration of vascular integrity in lung tissue. Additionally, MSCs suppress apoptosis, release growth cytokines, and stimulate cellular regeneration and differentiation in damaged lung areas^[49].

It has been documented that the paracrine secretion of MSCs serves a vital part in repair process of lung fibrosis by reducing inflammation and fibrosis. Furthermore, MSCs secrete immunosuppressive molecules that stimulate conversion of pro-inflammatory macrophages to anti-inflammatory ones. Additionally, MSCs secrete matrix metalloproteinase, an enzyme that directly breaks down the extracellular matrix, thereby facilitating the clearance of fibrosis^[50].

Whereas, PRP treated rats showed significant refinement of all the variables investigated versus lung fibrosis rats. However, the extent of improvement was not as significant as observed in those treated with BM-MSCs. Sections stained with H&E revealed some patent alveoli surrounded by thin alveolar septa, while others were collapsed or partially collapsed and separated by thickened alveolar walls. The alveoli were primarily lined by pneumocyte II cells, with only a few pneumocyte I cells present. Some detached epithelial cells were observed in the lumen of certain bronchioles. Moreover, there was moderate cellular infiltration of inflammatory cells around the bronchioles' adventitia and thickened walls of certain pulmonary blood vessels. These findings were in line with Maher *et al.*, 2020^[10], where his study showed that the lungs of the PRP treated group appeared relatively normal with peribronchiolar mononuclear inflammatory cell infiltration. EL-Shafei *et al.*, 2023^[51], also reported that PRP significantly improved cisplatin-induced cardiac damage.

These results were confirmed by significantly increased alveolar surface area and significantly decreased pneumocytes II prevalence in PRP group versus lung fibrosis group. PRP contains five to ten times higher levels of growth factors than in complete blood. Such factors are crucial for the regeneration of the injured area. Additionally, PRP inhibits the release of cytokines, thereby reducing inflammation^[10]. Furthermore, PRP maintains

the integrity of the pulmonary vasculature by stimulating angiogenesis, as well as stem cells multiplicity and distinction through paracrine and autocrine pathways^[52]. Moreover, PRP induces lung healing by promoting epithelial cell regeneration, relying on some epithelial stimulating factors like keratinocyte and hepatocyte growth factors^[54]. Furthermore, platelets possess anti-inflammatory properties as they inhibit the nuclear factor- κ B pathway and can actively circulate, forming complexes with other inflammatory and immune cells in various disorders^[51].

PRP treated group sections stained by Masson trichrome showed average collagen fibers deposition in the lung interstitium. This was supported by our histomorphometric results that showed significant reduction in collagen fibers percentage in PRP treated group versus lung fibrosis group. Antifibrosis action of PRP can be returned to its content of anti-fibrotic molecules, such as serum amyloid protein and hepatocyte growth factor, which have the ability to suppress fibrosis and regulate macrophage function^[51].

Going in line with previous findings, serum MDA and TGF-B1 level demonstrated a considerable decline versus lung fibrosis group. Similar results were reported by Maher *et al.*, 2020^[10], who observed significant decreased MDA in rats treated by PRP at the 5th and 6th weeks of the experiment in comparison to the lung fibrosis group.

Immunohistochemical analysis were also in line with the other findings of our study where immunostaining with α -SMA and CD68 antibodies revealed a significant reduction compared to the lung fibrosis group, indicating a decrease in fibrotic activity and macrophage infiltration. Regarding immunostaining with Bax, it also showed significant reduction in comparison to lung fibrosis group. Salem *et al.*, 2018^[53], demonstrated that PRP possesses an anti-apoptotic effect by reducing the mRNA level of caspase-3, while increasing the mRNA level of Bcl-2 protein (an anti-apoptotic regulator). These findings suggest that PRP holds promise as an approach for the treatment of various diseases.

CONCLUSION

This study demonstrated that amiodarone induced fibrosis in rat lungs. BM-MSCs and PRP significantly improved pulmonary fibrosis induced by amiodarone as proved by biochemical, histological and morphometric studies. The current findings demonstrated a more obvious improvement in response to BM-MSCs than PRP suggesting its possible future use as a therapeutic modality for attenuating lung fibrosis.

CONFLICT OF INTERESTS

There are no conflicts of interest.

REFERENCES

1. Zaghoul MS, Abdel-Salam RA, Said E, Suddek GM and Salem HAR. Attenuation of Bleomycin-induced pulmonary fibrosis in rats by flavocoxid treatment. *Egypt J Basic Appl Sci.* 2017; 4: 256-63. doi: 10.3390/molecules22040543.

2. King CS and Nathan SD. Idiopathic pulmonary fibrosis: effects and optimal management of comorbidities. *Lancet Respir Med.* 2017; 5: 72-84. doi: 10.1016/S2213-2600(16)30222-3.
 3. Wolters PJ, Blackwell TS, Eickelberg O, Loyd JE, Kaminski N, Jenkins G, Maher TM, Molina-Molina M, Noble PW, Raghu G, Richeldi L, Schwarz MI, Selman M, Wuyts WA and Schwartz DA. Time for a change: is idiopathic pulmonary fibrosis still idiopathic and only fibrotic? *Lancet Respir Med.* 2018; 6:154-60. doi: 10.1016/S2213-2600(18)30007-9.
 4. Raghu G, Rochwerg B, Zhang Y, Garcia CAC, Azuma A, Behr J, Brozek JL, Collard HR, Cunningham W, Homma S, Johkoh T, Martinez FJ, Myers J, Protzko SL, Richeldi L, Rind D, Selman M, Theodore A, Wells AU, Hoogsteden H, Schönemann HJ; American Thoracic Society; European Respiratory society; Japanese Respiratory Society; Latin American Thoracic Association. An official ATS/ERS/JRS/ALAT clinical practice guideline: treatment of idiopathic pulmonary fibrosis. An update of the 2011 clinical practice guideline. *Am J Resp Crit Care Med.* 2015; 192: 3-19. doi: 10.1164/rccm.201506-1063ST.
 5. Chu KA, Yeh CC, Kuo FH, Lin WR, Hsu CW, Chen TH and Fu YS. Comparison of reversal of rat pulmonary fibrosis of nintedanib, pirfenidone, and human umbilical mesenchymal stem cells from Wharton's jelly. *Stem Cell Res Ther.* 2020; 11: 513. doi: 10.1186/s13287-020-02012-y.
 6. Spagnolo P, Balestro E, Aliberti S, Cocconcelli E, Biondini D, Casa GD, Sverzellati N and Maher TM. Pulmonary fibrosis secondary to COVID-19: a call to arms? *Lancet Respir Med.* 2020; 8: 750-752. doi: 10.1016/S2213-2600(20)30222-8.
 7. Zakaria DM, Zahran NM, Arafa SA, Mehanna RA and Abdel-Moneim RA.. Histological and Physiological Studies of the Effect of Bone Marrow-Derived Mesenchymal Stem Cells on Bleomycin Induced Lung Fibrosis in Adult Albino Rats. *Tissue Eng Regen Med.* 2021; 18: 127-141. doi: 10.1007/s13770-020-00294-0.
 8. Bellou V, Belbasis L and Evangelou E. Tobacco Smoking and Risk for Pulmonary Fibrosis: A Prospective Cohort Study from the UK Biobank. *Chest.* 2021; 160: 983-993. doi: 10.1016/j.chest.2021.04.035.
 9. Ali EA, Abd El Salem EM, Daba MHY, Yassin AA, El kady NM, and Badr EA. The effect of atorvastatin on bleomycin- induced pulmonary fibrosis in rats. *Menoufia Med J.* 2018; 31: 1081-1087. doi: 10.4103/mmj.mmj_379_15.
 10. Maher ZM, Elsayed AA and Mohi El-Din MM: Clinicopathological Studies on the Remodeling Effect of Platelet-Rich Plasma on Lung Fibrosis Induced by Amiodarone in Albino Rats. *Veterinary Medicine and Public Health Journal.* 2020; 1: 108-114. doi:10.31559/VMPH2020.1.3.8.
 11. Ghabrial MMM, Salem MFM, El Ela AMAA, and El Deeb SAA. The possible therapeutic role of mesenchymal stem cells in amiodarone-induced lung injury in adult male albino rats. *Tanta Medical Journal.* 2018; 46: 172-182. doi: 10.4103/tmj.tmj_4_18.
 12. Young KA and Dilling DF. The Future of Lung Transplantation. *Chest.* 2019; 155: 465-473. doi: 10.1016/j.chest.2018.08.1036.
 13. Premer C, Schulman IH and Jackson JS. The role of mesenchymal stem/stromal cells in the acute clinical setting. *Am J Emerg Med.* 2021; 46: 572-578. doi: 10.1016/j.ajem.2020.11.035.
 14. Brown C, McKee C, Bakshi S, Walker K, Hakman E, Halassy S, Svinarich D, Dodds R, Govind CK, Chaudhry GR. Mesenchymal stem cells: Cell therapy and regeneration potential. *J Tissue Eng Regen Med.* 2019; 13: 1738-1755. doi: 10.1002/term.2914.
 15. Lana JFSD, Santana M, Belangero W and Luzo A (2014). "Platelet-rich plasma". *Lecture Notes in Bioengineering.* doi: 10.1007/978-3-642-40117-6.
 16. Collins T, Alexander D and Barkatali B. Platelet-rich plasma: a narrative review. *EFORT Open Rev.* 2021; 6: 225-235. doi: 10.1302/2058-5241.6.200017.
 17. Espina M, Jülke H, Brehm W, Ribitsch I, Winter K and Delling U. Evaluation of transport conditions for autologous bone marrow-derived mesenchymal stromal cells for therapeutic application in horses in PeerJ. 2016; 4: e1773. doi: 10.7717/peerj.1773.
 18. Kelp A, Abruzzese T, Wöhrle S, Frajs V and Aicher WK. Labeling Mesenchymal Stromal Cells with PKH26 or VybrantDil Significantly Diminishes their Migration, but does not affect their Viability, Attachment, Proliferation and Differentiation Capacities. *J Tissue Sci Eng.* 2017; 10: 8-199. doi: 10.4172/2157-7552.1000199.
 19. Saba AI, Elbakary RH, Afifi OK and Sharaf Eldin HEM. Effects of Platelet-Rich Plasma on the Oxymetholone-Induced Testicular Toxicity. *Diseases.* 2023; 11: 84. doi: 10.3390/diseases11020084.
 20. Pourghasem M, Nasiri E and Shafi H. Early renal histological changes in alloxan-induced diabetic rats. *Int J Mol Cell Med.* 2014; 3: 11-5. doi:PMC3927393.
 21. Kuru K. Optimization and enhancement of H and E stained microscopical images by applying bilinear interpolation method on lab color mode. *Theoretical Biology and Medical Modelling.* 2014; 11:9-18. doi: 10.1186/1742-4682-11-9.
 22. Suvarna K, Layton C and Bancroft J. *Theory and Practice of Histological Techniques.* Seventh ed. Churchill living-stone of el sevier, Philadelphia, USA. 2013, 173-214. <https://doi.org/10.1016/B978-0-7020-4226-3.00010-X>.
-

23. García-Sáez AJ. The secrets of the Bcl-2 family. *Cell Death and Differentiation*. 2012; 19: 1733-1740. doi: 10.1038/cdd.2012.105.
24. Emsley R, Dunn G and White IR: Mediation and moderation of treatment effects in randomized controlled trials of complex interventions in *Stat Methods Med Res*. 2010; 19: 237-270. doi: 10.1177/0962280209105014.
25. Zhao X, Kwan JYY, Yip K, Liu PP and Liu FF. Targeting metabolic dysregulation for fibrosis therapy. *Nat Rev Drug Discov*. 2020 ;19: 57-75. doi: 10.1038/s41573-019-0040-5.
26. Mansouri N, Willis G, Fernandez-Gonzalez A, Reis M, Mitsialis A and Kourembanas S. Mesenchymal stem cell exosomes ameliorate experimental idiopathic pulmonary fibrosis by modulating alveolar macrophage phenotype and monocyte recruitment. In: D97 If you love it, let it go: Exosomes and secretomes. *American Thoracic Society*. 2018. 4(21):e128060. doi: 10.1172/jci.insight.128060.
27. Knight AD and Kacker S. Platelet-Rich Plasma Treatment for Chronic Respiratory Disease. *Cureus*. 2023 ;15: e33265. doi:10.7759/cureus.33265.
28. Terzo, F.; Ricci, A.; D'Ascanio, M.; Raffa, S. and Mariotta, S. Amiodarone-induced pulmonary toxicity with an excellent response to treatment: A case report. *Respir. Med. Case Rep*. 2020; 29: 100974. doi: 10.1016/j.rmcr.2019.100974.
29. Hasan, H. F., Thabet, N. M. and Abdel-Rafei, M. K. Methanolic extract of moringa oleifera leaf and low doses of gamma radiation alleviated amiodarone induced lung toxicity in albino rats. *Arch. Biol. Sci*. 2016; 68: 31-39. doi:10.2298/ABS150729005H.
30. Gawad FA, Rizk A, Jouakim MF and Halem MZAE. Amiodarone-induced lung toxicity and the protective role of Vitamin E in adult male albino rat. *European Journal of Anatomy*. 2018; 22: 323-333. doi: eja.170419ar.
31. Ingale P, Rai P, Salunkhe V and Awad N. Is Malondialdehyde (MDA) used as a Oxidative Stress Marker in Chronic Obstructive Pulmonary Disease (COPD) andamp; Cigarette Smokers. *JK Science*. 2022; 24(2):239-42. <https://journal.jkscience.org/index.php/JK-Science/article/view/155>.
32. Chen G, Sun L, Kato T, Okuda K, Mar tino MB, Abzhanova A, Lin JM, Gilmore RC, Batson BD, O'Neal YK, Volmer AS, Dang H, Deng Y, Randell SH, Button B, Livraghi-Butrico A, Kesimer M, Ribeiro CM, O'Neal WK and Boucher RC. IL-1 β dominates the promucin secretory cytokine profile in cystic fibrosis. *J Clin Invest*. 2019;129: 4433-4450. doi: 10.1172/JCI125669.
33. Hinz, B. and Lagares, D. Evasion of apoptosis by myofibroblasts: a hallmark of fibrotic diseases. *Nat. Rev. Rheumatol*. 2020; 16:11–31. doi: 10.1038/s41584-019-0324-5.
34. Al-Shammari B, Khalifa M, Bakheet SA, Yasser M. A Mechanistic Study on the Amiodarone-Induced Pulmonary Toxicity. *Oxid Med Cell Longev*. 2016; 2016: 1-10. doi: 10.1155/2016/6265853.
35. Moustafa DE, Youssef MY and Emam NM. Oxidative Stress in Amiodarone-Induced Pulmonary Toxicity in Rats and the Protective Effect of L-carnitine and Vitamin C. *Mansoura J. Forens. Med. Clin. Toxicol*. 2020; 28: 43-52. doi:10.21608/mjfmct.2020.19954.1006.
36. Anversa P, Kajstura J, Leri A, Loscalzo J. Tissue-specific adult stem cells in the human lung. *Nat Med*. 2011; 17: 1038-1039. doi: 10.1038/nm.2463.
37. Adams TS, Schupp JC, Poli S, Ayaub EA, Neumark N, Ahangari F, Chu SG, Raby BA, DeJuliis G, Januszyk M, Duan Q, Arnett HA, Siddiqui A, Washko GR, Homer R, Yan X, Rosas IO and Kaminski N. Single-cell RNA-seq reveals ectopic and aberrant lung-resident cell populations in idiopathic pulmonary fibrosis. *Sci Adv*. 2020; 6(28). doi: 10.1126/sciadv.aba1983.
38. Ramachandran P, Dobie R, Wilson-Kanamori JR, Dora EF, Henderson BEP, Luu NT, Portman JR, Matchett KP, Brice M, Marwick JA, Taylor RS, Efremova M, Vento-Tormo R, Carragher NO, Kendall TJ, Fallowfield JA, Harrison EM, Mole DJ, Wigmore SJ, Newsome PN, Weston CJ, Iredale JP, Tacke F, Pollard JW, Ponting CP, Marioni JC, Teichmann SA and Henderson NC. Resolving the fibrotic niche of human liver cirrhosis at single-cell level. *Nature*. 2019; 575: 512-518. doi: 10.1038/s41586-019-1631-3.
39. Allawzi A, Elajaili H, Redente EF, and Nozik-Grayck E. Oxidative toxicology of bleomycin: role of the extracellular redox environment. *Curr Opin Toxicol*. 2019; 13: 68–73. doi: 10.1016/j.cotox.2018.08.001.
40. Zhang L, Wang Y, Wu G, Xiong W, Gu W, Wang CY. Macrophages: friend or foe in idiopathic pulmonary fibrosis? *Respir Res*. 2018; 19: 170. doi: 10.1186/s12931-018-0864-2.
41. Hughes KT, Beasley MB. Pulmonary manifestations of acute lung injury: more than just diffuse alveolar damage. *Arch Pathol Lab Med*. 2017; 141: 916–22. doi: 10.5858/arpa.2016-0342-RA.
42. Kim MS, Baek AR, Lee JH, Jang AS, Kim DJ, Chin SS, *et al*. IL-37 attenuates lung fibrosis by inducing autophagy and regulating TGF- β 1 production in mice. *J Immunol*. 2019; 203: 2265–75. doi: 10.4049/jimmunol.1801515.

43. Dong SH, Liu YW, Wei F, Tan HZ, Han ZD. Asiatic acid ameliorates pulmonary fibrosis induced by bleomycin (BLM) via suppressing pro-fibrotic and inflammatory signaling pathways. *Biomed Pharmacother.* 2017; 89:1297–309. doi: 10.1016/j.biopha.2017.03.005.
44. Ma, B. N., and Li, X. J. Resveratrol extracted from Chinese herbal medicines: A novel therapeutic strategy for lung diseases. *Chin. Herb. Med.* 2020; 12: 349–358. doi: 10.1016/j.chmed.2020.07.003.
45. Plataki, M., Koutsopoulos, A. V., Darivianaki, K., Delides, G., Siafakas, N. M. and Bouros, D. Expression of apoptotic and antiapoptotic markers in epithelial cells in idiopathic pulmonary fibrosis. *Chest.* 2005; 127: 266-274. doi: 10.1378/chest.127.1.266.
46. Lescoat A, Lelong M, Jeljeli M, Piquet-Pellorce C, Morzadec C, Ballerie A, Jouneau S, Jego P, Vernhet L, Batteux F, Fardel O and Lecureur V. Combined anti-fibrotic and anti-inflammatory properties of JAK-inhibitors on macrophages *in vitro* and *in vivo*: Perspectives for scleroderma-associated interstitial lung disease. *Biochem Pharmacol.* 2020; 178:114103. doi: 10.1016/j.bcp.2020.114103.
47. Hamam, Mostafa HKK and Raafat MH. Histological Study on Possible Therapeutic Effect of BM-MSCs on Healing of Lung Fibrosis Induced by CCl4 with Reference to Macrophage Plasticity. *J Cytol Histol.* 2019; 10: 537. doi:10.4172/2157-7099.1000537.
48. Sabry MM, Elkalawy SA, Abo-Elmour RK and Abd-El-Maksod DF. Histological and immunohistochemical study on the effect of stem cell therapy on bleomycin induced pulmonary fibrosis in albino rat. *Int J Stem Cells.* 2014; 7: 33-42. doi: 10.15283/ijsc.2014.7.1.33.
49. Savukinas UB, Enes SR, Sjoland AA and Westergren-Thorsson G. Concise review: the bystander effect: mesenchymal stem cell-mediated lung repair. *Stem Cells.* 2016; 34:1437–1444. doi: 10.1002/stem.2357.
50. Abdel Halim AS, Ahmed HH, Aglan HA, Abdel Hamid FF and Mohamed MR. Role of bone marrow-derived mesenchymal stem cells in alleviating pulmonary epithelium damage and extracellular matrix remodeling in a rat model of lung fibrosis induced by amiodarone. *Biotech Histochem.* 2021; 96: 418-430. doi: 10.1080/10520295.2020.1814966.
51. El-Shafei, A., Hassan, R., Hosny, S. A Comparative Histological and Immunohistochemical Study on the Possible Therapeutic Effects of Empagliflozin and platelet-rich plasma Against Cisplatin Induced Cardiotoxicity in Rats. *Egyptian Journal of Histology.* 2023; 46 :378-493. doi: 10.21608/EJH.2021.69267.1451.
52. Mammoto T, Jiang A, Jiang E and Mammoto A. Platelet rich plasma extract promotes angiogenesis through the angiopoietin1-Tie2 pathway. *Microvasc Res.* 2013; 89: 15-24. doi: 10.1016/j.mvr.2013.04.008.
53. Zhang J, Middleton KK, Fu FH, Im HJ and Wang JH. HGF mediates the anti-inflammatory effects of PRP on injured tendons. 2013; 8: e67303. doi: 10.1371/journal.pone.0067303.
54. Salem N, Hamza A, Alnahdi H and Ayaz N: Biochemical and Molecular Mechanisms of Platelet-Rich Plasma in Ameliorating Liver Fibrosis Induced by Dimethylnitrosurea in Cell Physiol Biochem. 2018; 47: 2331-2339. doi: 10.1159/000491544.

الملخص العربي

التأثير العلاجي للخلايا الجذعية المستخلصة من نخاع العظام مقابل البلازما الغنية بالصفائح الدموية على تليف الرئة المحدث بالاميويدارون في ذكر الجرذ الأبيض البالغ: دراسة هستولوجية

وفاء عبد العظيم عبده بغدادى، زينب حجاب، دينا هشام محمد

قسم الهستولوجيا، كلية الطب، جامعة القاهرة، القاهرة، مصر

المقدمة: يعد تليف الرئة واحد من الامراض التدريجية الخطيرة الغير منعكسة والمنتشرة في كل انحاء العالم. فهو يسبب تدهور تدريجى في وظيفة الرئة ثم فشل تنفسى يستلزم زراعة رئة. يعتبر الاميويدارون دواء فعال مضاد لعدم انتظام ضربات القلب والذى يسبب اثار جانبية عديدة على الرئة، ومن اخطرها تليف الرئة. حديثا، ظهرت الخلايا الجذعية والبلازما الغنية بالصفائح الدموية كواحدتان من الأدوات العلاجية البديلة الواعدة التي يمكن ان تحل محل زراعة الاعضاء بكل عيوبها.

الهدف من البحث: مقارنة التأثير العلاجي للخلايا الجذعية المستخلصة من نخاع العظام مقابل البلازما الغنية بالصفائح الدموية على تليف الرئة المحدث بعقار الاميويدارون في نموذج ذكر الجرذ البالغ

المواد وطرق البحث: تم تقسيم ثلاثة وخمسين فار الى اربع مجموعات بالإضافة الى المجموعة المانحة، والتي تشمل: المجموعة الأولى (الضابطة)، المجموعة الثانية (تليف الرئة) والتي تم حقنها بالاميويدارون (٨٠ مجم / كجم) في البطن يوميا لمدة اربع أسابيع، المجموعة الثالثة (الخلايا الجذعية المستخلصة من نخاع العظام) والتي تم معاملة مثل المجموعة الثانية ثم تم حقنها في الوريد بواحد مل من الخلايا الجذعية كجرعة واحدة ثم تركت لمدة اربع أسابيع والمجموعة الرابعة (البلازما الغنية بالصفائح الدموية) والتي عوملت مثل المجموعة الثانية ثم تم حقنها في البطن بالبلازما الغنية بالصفائح الدموية (٠,٥ مل / كجم) مرتين أسبوعيا لمدة اربع أسابيع. تم قياس مستوى المالونديالدهيد و عامل النمو المحول بيتا في المصل وتم صبغ قطاعات الرئة بالهيماتوكسيلين والإيوسين وصبغة ماسون ثلاثية الألوان والصبغة الهستوكيميائية المناعية ضد الألفا اكتين الخاص بالعضلات الملساء و Bax و عنقود التمايز ٦٨ (CD ٦٨) و ايضا تم عمل القياسات المترية الشكلية و التحليل الاحصائى.

النتائج: أظهرت المجموعة الثانية الملامح الهستولوجية المطابقة لتليف الرئة وتركيب ومؤشرات بيوكيميائية وقياسات مترية شكلية غير طبيعية. بينما أظهرت المجموعتان الثالثة والرابعة تحسنا ملحوظا وتحسنا جزئيا على التوالي في التركيب الهستولوجى والمؤشرات البيوكيميائية والقياسات المترية الشكلية.

الاستنتاج: أثبتت الخلايا الجذعية المستخلصة من نخاع العظام انها علاج اكثر فاعلية لتليف الرئة من البلازما الغنية بالصفائح الدموية وذلك يرجع الى آثارها المجددة للخلايا والمضادة للالتهاب والموت الخلوى المبرمج.